recovery energy environment economy
2011 CSPG CSEG CWLS Convention

CO_2 Rock Physics: A Laboratory Study

Helen Yam*
University of Alberta, Edmonton, Alberta, Canada
hyam@ualberta.ca
and
Douglas R. Schmitt
University of Alberta, Edmonton, Alberta, Canada

Summary

It is expected that 4D seismic monitoring will play a critical role in monitoring geologically sequestered CO_2 but understanding the seismic rock physics of sequestered CO_2 remains a key knowledge gap. Ultrasonic pulse transmission experiments were conducted on a fully CO_2 saturated porous ceramic rod subjected to a range of pressures and temperatures that crosses the CO_2 phase boundaries between gas, liquid, and supercritical, such pore fluid conditions are found within the uppermost kilometer of most sedimentary basin. P- and S-wave velocities and differential attenuation coefficients were determined from the laboratory data. The measured elastic wave velocities showed good agreement with Biot's model where as the measured differential attenuation coefficient showed similar trends with changing pore pressure and frequencies, but is 6-7 times greater in absolute value.

Introduction

Main concerns in geological CO_2 sequestration are whether the injected CO_2 will stay in place over time, and the ability to observe and verify the injected CO_2 from the surface (Benson, 2006; Chadwick et al, 2009). Therefore, monitoring the subsurface movement and phase behavior of the injected CO_2 is a crucial aspect of any carbon capture and storage project. Due to the sensitivity of seismic waves to pore fluid contents, time lapse seismology is regarded as a promising monitoring method for geological CO_2 sequestration projects (Benson and Surles, 2006) and is employed in all industrial scale projects (Sleipner, Weyburn, In Salah). To utilize seismic methods effectively as a monitoring tool, it is therefore essential to understand the effect of CO_2 as a pore fluid on the overall rock seismic response. Laboratory work using a fully saturated synthetic sample has been conducted for a variety of temperatures and pressures that are representative of subsurface conditions in which CO_2 can be in gas, liquid, supercritical fluid phases. This is particularly important in seismic monitoring as CO_2 transformations can occur at quite modest temperatures and pore pressures; all three phases are readily obtained within the uppermost kilometer of a sedimentary basin. Elastic wave velocity variations and wave strength dampening are observed with phase transitions, signifying that the physical property changes of the pore fluid due to changing in situ conditions can be detected using seismic. Although full CO_2 saturation is not expected as in real cases in the earth the pore space would also contain brine or hydrocarbons, this work provides an end member understanding in the evolution of seismic responses resulting from changes in the phase state of CO_2.

CO_2 elastic properties and behaviours

Figure 1 displays the bulk modulus and density phase diagrams of CO_2 as a function of pressure and temperature based on the thermodynamic model of Span and Wagner (1996). The accepted critical point of CO_2 is at 31° C and at 7.4 MPa. Below this pressure and temperature, CO_2 can be either a gas or liquid in respect of the possible subsurface conditions. The vapor-liquid boundary is clearly marked by an abrupt change in the physical properties of CO_2 where this sudden change disappears as the critical point is reached and denotes the beginning of the supercritical fluid phase state. A main characteristic of supercritical fluids is that it has physical behaviors of both a gas and a liquid. As a consequence of this characteristic, any gas or liquid phase transitions into the supercritical phase results in a smooth variation, unlike the gas to liquid transition.

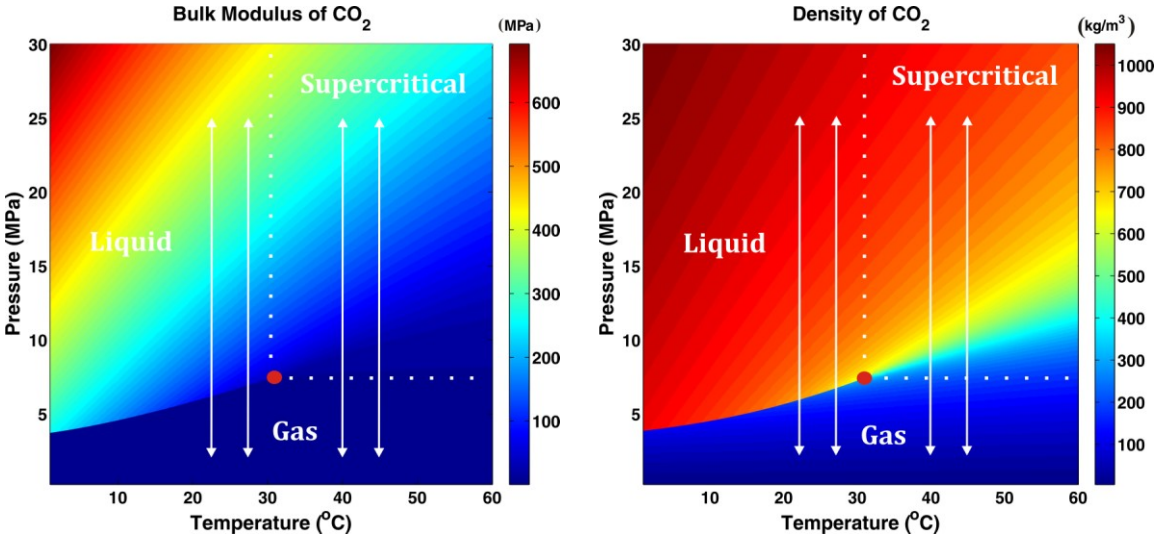

Figure 1: Bulk modulus (left) and density (right) phase diagrams of CO2. The red dot on both phase diagrams marks the critical point of CO_2. The vapor-liquid boundary is clearly discernible from the sudden change in physical properties. The boundaries of the supercritical fluid phase state are marked by the white dotted line. The white arrows shows the temperature and pressure conditions applied to the CO_2 during ultrasonic pulse transmission measurements.

Experiment

A porous ceramic rod, derived from a high fired alumina body (Al_2O_3) was used as the host sample in this study. This sample has a porosity of 58%, with an air permeability of about 100mD. This synthetic sample was chosen for this study because of its lack of microcracks, which can complicate the acoustic behavior of real rocks. Although this sample is extremely porous and is not reflective of real reservoir rocks, its large porosity will allow the overall rock behavior to be more susceptible to the changes in the physical properties of the pore fluid. This reinforces the purpose of our work on establishing an extreme end member understanding on the rock physics involved with CO_2 as the pore fluid.

Ultrasonic pulse transmission method was applied to determine the elastic behavior of the sample. A cylindrical sample 50 mm in length and 25.4 mm in diameter was placed in between a transmitting and a receiving transducer made of P- and S- piezoelectric ceramics with center frequencies of 1MHz mounted on an aluminum buffer cap. The sample-transducer assembly was set inside a pressure vessel that was filled with hydraulic oil as the hydrostatic pressure medium. The sample was jacketed in a Tygon® tube, a flexible clear plastic to seal it from hydraulic oil contamination. CO_2 is introduced into the initially dry and vacuumed sample from pressure bottle of hospital grade CO_2 located outside the vessel. An electrical resistance tape is wrapped around the outside of the vessel and controls the temperature of the experiment and is measured by K-type thermocouple placed inside the pressure vessel.

The transmitted signal is generated by exciting the transmitting transducer with a fast-rising 200 V square wave from a pulse generator. The propagated signal was recorded by a digital oscilloscope system at a sampling rate of 10 nanoseconds. The final waveform is a stack of over 500 traces to reduce random noise effects. From the final waveforms the transit time of the signals can be deduced, and with the length of the sample the elastic wave velocities can be calculated. The general scheme of the experiment is shown in figure 2.

Ultrasonic measurements were made on the sample under dry and CO_2 saturated conditions. The dry measurements were done with the pore space under vacuum (Pp =0 MPa) while the confining pressure varied from 2 MPa to 40 MPa. The resulting elastic wave velocities showed no differential pressure dependence due to the lack of microcracks. For the CO_2 saturated measurements, 4 different constant temperature runs were conducted while pore pressure varied from 2 MPa to 25 MPa. The constant temperature runs were done at 23° C, 28° C, 40° C, and 45° C. For each measurement run, a constant differential pressure of 15 MPa was maintained by varying the confining pressure accordingly to the pore pressure. In figure 1, superimposed on the phase diagrams of CO_2 are the different temperatures and pore pressures conditions explored during the series of CO_2 saturated measurements. As pore pressure increases, for the lower temperature runs (23°C and 28°C), CO_2 changes from a gas phase to a liquid phase while for the higher temperature runs (40°C and 45°C), CO_2 changes from a gas phase to the supercritical fluid phase.

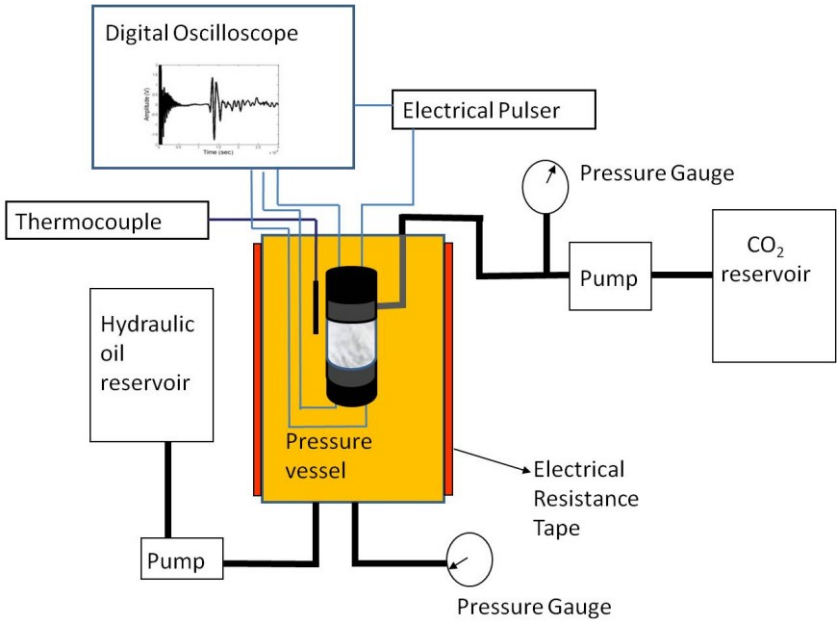

Figure 2: Experimental setup for ultrasonic pulse transmission for CO2 saturated measurements.

Examples

Figure 3 shows the P- and S-wave waveforms recorded for one of the lower temperature and one of the high temperature runs, T=28° C and T=40° C, respectively. The variations of the waveforms with pore pressure for the T = 23° C run is similar to T = 28° C run and so is T = 45° C run with T = 40° C run, and therefore they are not shown to avoid redundancy. The phase transition out of the gaseous phase state as pore pressure increases are all marked by a slower arriving and weakened P- and S-wave signal. The change is more drastic for the lower temperature runs and is related to the sharp contrast in gas to liquid physical properties see in the bulk modulus and the density phase diagrams of CO_2. The transition for the higher temperature runs is less abrupt and occurs at a higher pore pressure as expected since the critical pressure marks the limit of the vapor-liquid boundary.

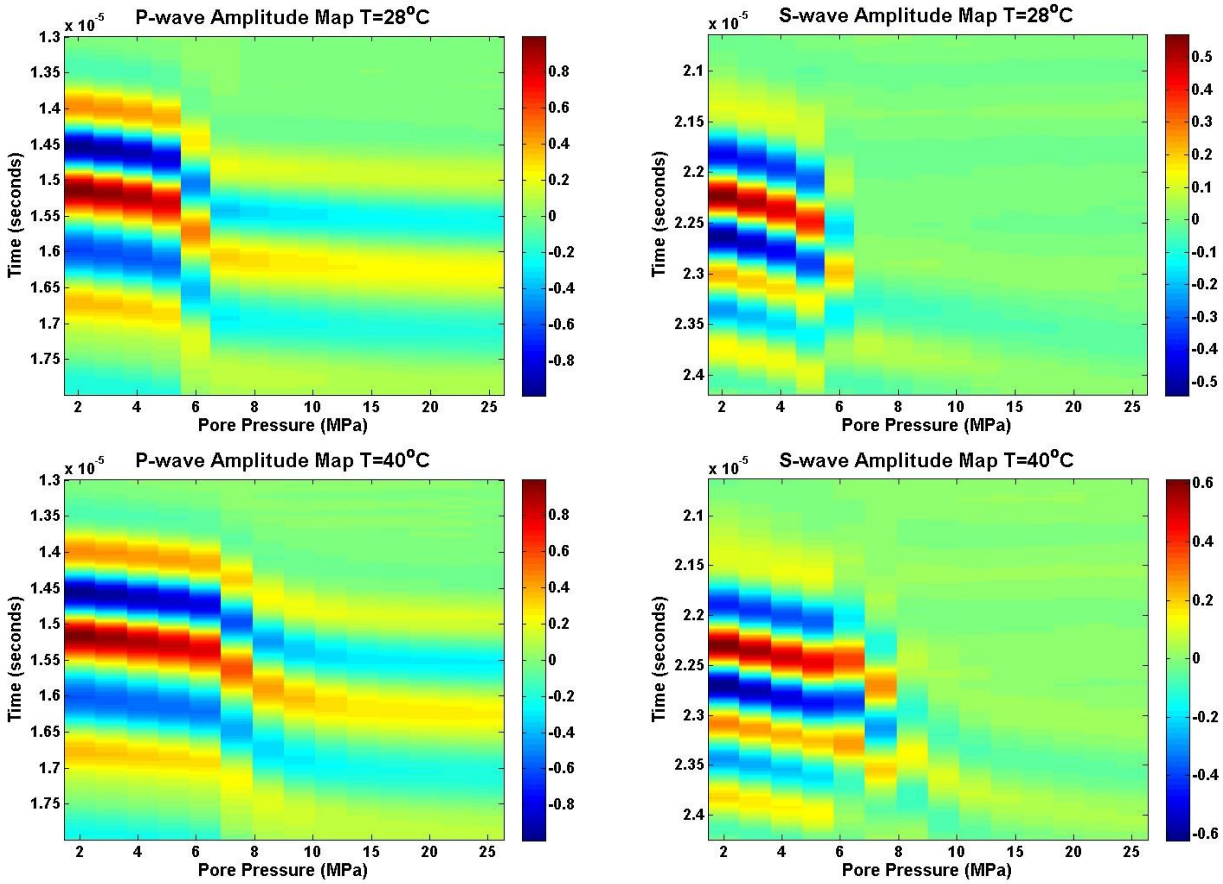

Figure 3: P- and S-wave (left and right, respectively) waveforms collected for T=28° C and T=40° C (top and bottom, respectively) constant temperature runs.

From analyzing the above waveforms, the P-and S-wave velocities are determined and displayed in figure 4. On these plots, the velocity of the dry sample at a differential pressure of 15MPa is shown by the black dot. Once CO_2 is introduced into the pore space, irrespective of the phase state of the CO_2, the elastic waves traveling through the sample are slower than when the pore space is at vacuum. In each constant temperature run the CO_2 phase change is marked by a drop in both P- and S-wave velocity of 4-5%, with the drop being more gradual for the higher temperature runs. Within a given phase state (gas, liquid, or supercritical fluid), as pore pressure increases the elastic wave velocities lessens and this is due to the increased density experienced.

Apart from velocity analyses, attenuation analyses have also been done on the waveforms acquired. Figure 5 shows the differential attenuation coefficients for the constant temperature runs of T=28° C and T=40° C as a function of pore pressure and frequency. Differential attenuation coefficient is the attenuation coefficient of each signal minus the attenuation coefficient of the signal when Pp=2MPa of that measurement run. The signal of Pp=2MPa was used because it is the least attenuated signal of the set of signals. The advantages of dealing with differential attenuation coefficients over the conventional method of determining absolute attenuation coefficients is that the former requires less time and uses only one sample, while the purpose of demonstrating signal strength variation is still preserved.

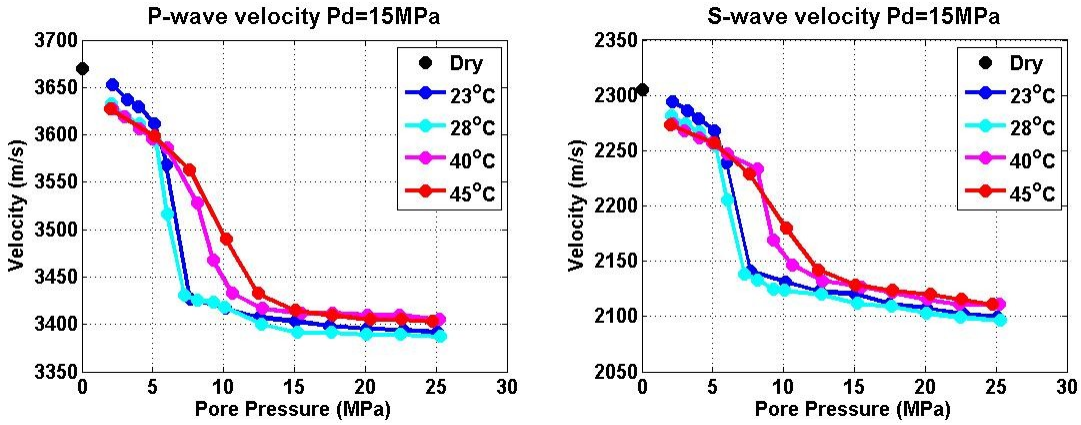

Figure 4: Ultrasonic P- and S-wave (left and right, respectively) velocities measured of the sample saturated with CO2 under various temperatures and pore pressures and when the sample is not saturated (black dot at Pp=0MPa). All measurements on the two plots were completed with a differential pressure of 15MPa. The error of the P-and S-wave velocities is about the size of the marker.

In all plots of figure 5, two general trends of the differential attenuation coefficient can be noted. First, the differential attenuation coefficients is the lowest at low pore pressures (gaseous phase state) and increases at high pore pressures (liquid or supercritical), which is anticipated based on the variations of the waveforms observed in figure 3. Second, higher frequencies are more attenuated than lower frequencies especially at higher pore pressures; Q is not constant over this range of frequencies.

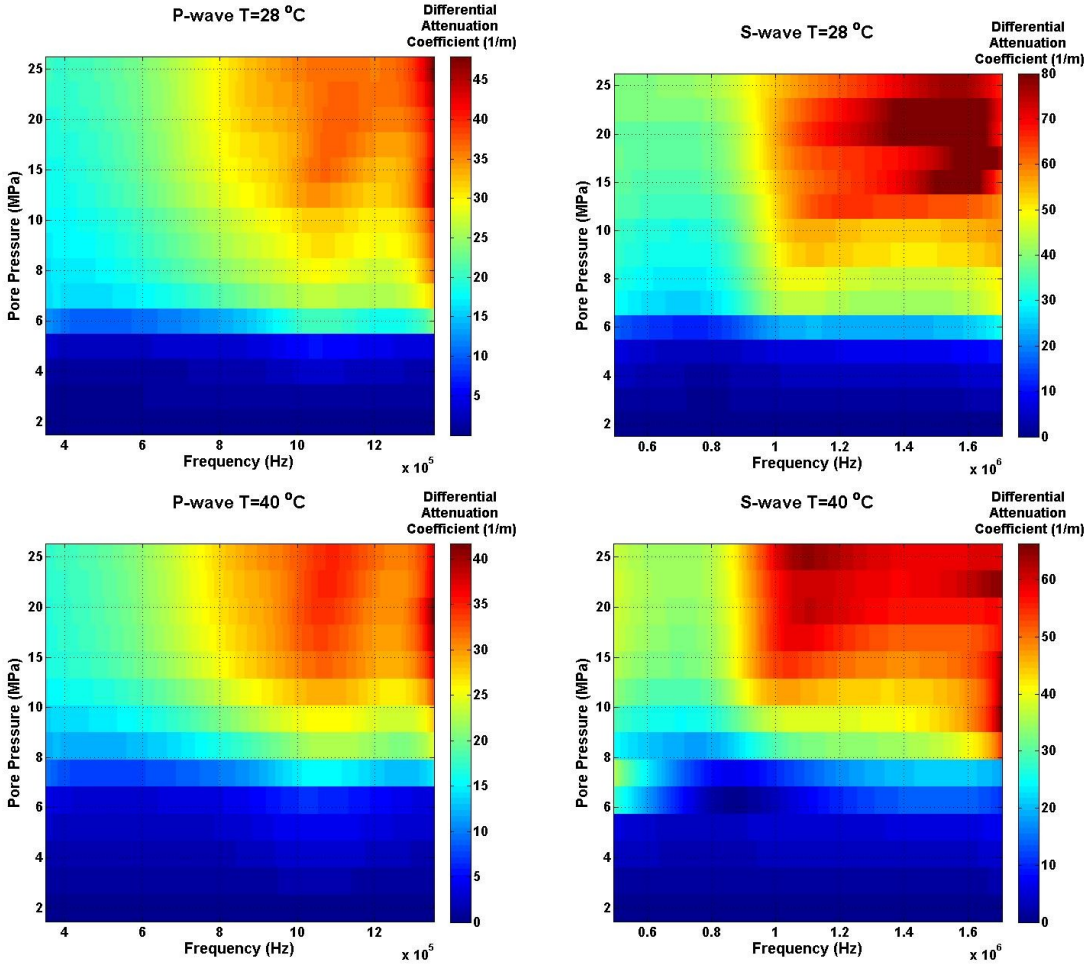

Figure 5: Differential attenuation coefficient of P- and S-wave (left and right, respectively) for T=28° C and T=40° C (top and bottom, respectively) constant temperature runs from laboratory data.

For the S-wave plot of T=28° C, there is large variability of the differential attenuation coefficient at the top right corner corresponding to high pore pressure and high frequencies and this is caused by noise effects. The more attenuated a signal is, the smaller the signal will be and the more susceptible it is to the effects of noise.

It is important to compare the laboratory results to rock physics models to see whether the responses can be predicted from existing theories; this is particularly true should we wish to make predictions of behaviour at typical seismic frequencies (~5 Hz to 300 Hz). If the responses can be predicted, then other signal responses can be determined for various conditions without replicating it in the laboratory. Biot's theory (see Bouzidi and Schmitt, 2009) was used to model the signal response under the same conditions applied in the laboratory by using the fluid properties from Span and Wagner's CO_2 thermodynamic model and the sample dry bulk and shear moduli characterized from the porous ceramic rod. The modeled P- and S-wave velocities using Biot's equations are shown in figure 6. There is excellent agreement of the modeled and laboratory measured Biot fast P and the shear wave velocities. Figure 7 shows the modeled differential attenuation coefficient over the same frequency interval, temperature and pore pressure conditions as analyzed with the laboratory data. The two general trends observed in figure 5 with respect to pore pressure and frequency is also seen in figure 7. However the trends from Biot's model appear more linear than what is observed with our data. In addition, when comparing the actual values of the differential attenuation coefficients, the modeled values are about 6-7 times less than the measured values from laboratory data.

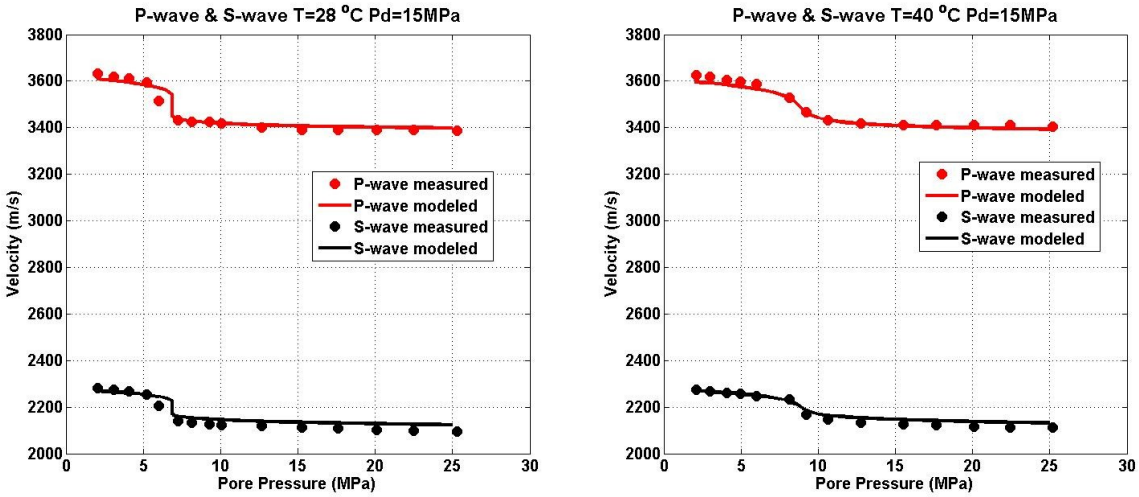

Figure 6: P- and S-wave velocities measured in the laboratory (dots) and modeled from Biot's theory (solid lines) for T=28° C and T=40° C constant temperature runs.

Conclusions

P- and S-wave laboratory data were acquired for various pressure and temperature conditions in a porous ceramic rod. Results show clear variations of elastic wave velocities and differential attenuation coefficient with the phase transitions of CO_2. Biot's model was used to replicate the elastic wave velocities and differential attenuation coefficient. There is good agreement for the P-and S-wave velocities but not for the differential attenuation coefficient. However, the general trend with pore pressure and frequency is in agreement. These results show that elastic waves are sensitive to changes in the pore space and CO_2 phase change is evident from signal variations. However these results are for an extreme end member, and they do not imply the same results can be attained with a real rock that is less porous, and may contain more than just CO_2 in the pore fluid.

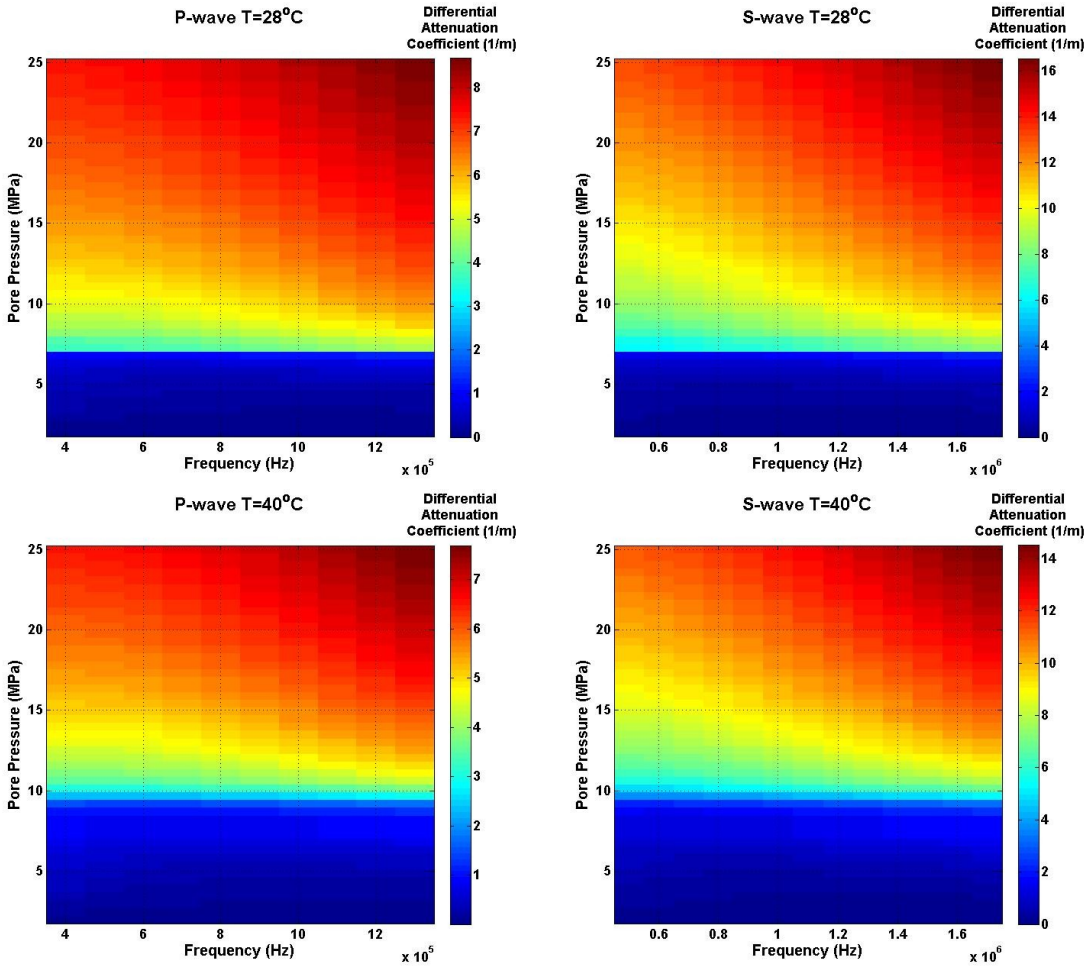

Figure 7: Differential attenuation coefficient of P- and S-wave (left and right, respectively) for T=28° C and T=40° C (top and bottom, respectively) constant temperature runs from Biot's theory.

Acknowledgements

HY would like to thank the NSERC-CGS M.Sc. award for support, and the NSERC Discovery Program for support of the laboratory work and purchase of some of the equipment that allowed us to appropriately control fluid pressures in the samples. Also,a big thanks to UofA Physics Dept. technicians, Len Tober and Lucas Duerksen for their technical support in making these experiments possible.

References

Benson, S. M., 2006, Monitoring Carbon dioxide sequestration in deep geological formations for inventory verification and carbon credits, 2006 SPE Annual Technical Conference and Exhibition in San Antonio, USA, 24-27 September 2006.

Benson, S. M., and Surles, T., 2006, Carbon dioxide capture and storage: An overview with emphasis on capture and storage in deep geological formations, Proceedings of the IEEE, **94**, 1795-1805.

Bouzidi, Y., and Schmitt, D. R., 2009, Measurement of the speed and attenuation of the Biot slow wave using a large ultrasonic transmitter, J. Geophys. Res., **114**, B08201.

Chadwick, R. A., Arts, R., Bentham, M., Eiken, O., Holloway, S., Kirby, G. A., Pearce, J.M., Williamson, J. P., Zweigel, P., 2009, Review of monitoring issues and technologies associated with the long-term underground storage of carbon dioxide (in Underground gas storage; worldwide experiences and future development in the UK and Europe): Geological Society of London Special Publications, **313**, 257-275.

Span, R., and Wagner, W.,1996, A new equation of state for carbon dioxide covering the fluid region from the triple-point temperature to 1100 K at pressures up to 800 MPa, J. Phys. Chem. Ref. Data, ***25***, 1509-1596.